Origin, distribution and environmental significance of perylene in Okinawa Trough since last glaciation maximum

Xinyu Zhang [a], Yunping Xu [a,b,*], Jiaping Ruan [a], Su Ding [a], Xianyu Huang [c]

[a] MOE Key Laboratory for Earth Surface Processes, College of Urban & Environmental Sciences, Peking University, Beijing 100871, China
[b] Qingdao Collaborative Innovation Center of Marine Science and Technology, Qingdao 266003, China
[c] Department of Geography, Faculty of Earth Sciences, China University of Geosciences, Wuhan, Hubei 430074, China

ABSTRACT

Perylene, a five-ring nuclear polycyclic aromatic hydrocarbon (PAH), has a different distribution pattern from anthropogenic PAHs. Its source, however, remains obscure, limiting its application as an environmental indicator. Here we examine perylene in the upper 85 m sediments of the ODP Hole 1202B from the southern Okinawa Trough. Over the past 20,000 years, the mass accumulation rate of perylene is substantially higher in the last deglaciation than the Holocene and last glacial maximum. Perylene presents a strong correlation with C_{31} n-alkane ($r = 0.55$; $p < 0.001$), a biomarker for terrigenous organic matter, and a weak correlation with $C_{37:2}$ alkenone ($r = -0.04$; $p = 0.23$), a biomarker for marine organic matter. The mean $\delta^{13}C$ value of perylene ($-22.8‰ \pm 0.6‰$) is substantially higher than that of long chain n-alkanes ($-30.7 \pm 0.4‰$), but close to that of fluvial organic matter in adjacent areas ($-24.0‰$ to $-25.0‰$). Our results strongly suggest that the perylene is of a terrigenous origin likely from soil fungi, and may be a useful tracer for soil organic carbon in marine environments.

© 2014 Elsevier Ltd. All rights reserved.

1. Introduction

Polycyclic aromatic hydrocarbons (PAHs) have attracted intensive attention because of their toxic, carcinogenic and mutagenic properties. Like other PAHs, perylene ($C_{10}H_{12}$) is widely distributed in recent environments such as soils/peats (e.g., Wilcke et al., 2003; Gocht et al., 2007), lake sediments (e.g., Ishiwatari et al., 1980; Gschwend and Hites, 1981; Silliman et al., 1998, 2001; Itoh and Hanari, 2010; Fan et al., 2011) and marine sediments (e.g., Orr and Grady, 1967; Aizenshtat, 1973; Laflamme and Hites, 1978; Wakeham et al., 1979; Gschwend and Hites, 1981; Gschwend et al., 1983; Silliman et al., 2000; Soclo et al., 2000) as well as ancient deposits such as coal, oil and sedimentary rocks (e.g., Louda and Baker, 1984; Jiang et al., 2000; Grice et al., 2009). However, the distribution profile of perylene is distinctly different from that of other PAHs. Firstly, perylene is the dominant PAH in many pristine environments, but only a small amount (< 10% of total PAHs) in contaminated aerosols, soils and sediments (Baumard et al., 1998; Jiang et al., 2000; Silliman et al., 2000). Secondly, the perylene concentration usually increases with depth, whereas other PAHs dramatically decline in deeper sediments (Orr and Grady, 1967; Aizenshtat, 1973; Ishiwatari et al., 1980; Wakeham et al., 1980; Silliman et al., 1998; Fan et al., 2011). These facts suggest that perylene and other PAHs have different sources or environmental processes (Aizenshtat, 1973; Silliman et al., 2000; Itoh and Hanari, 2010).

Nowadays, it is generally accepted that perylene is mainly a diagenetic product derived from natural precursors (Aizenshtat, 1973; Venkatesan, 1988; Silliman et al., 1998, 2000; Itoh and Hanari, 2010). However, there is no consensus yet as to whether perylene is of a terrigenous or aquatic origin. Perylene has been found in marine sediments without significant terrigenous inputs, supporting an aquatic origin (e.g., diatoms) for perylene (Orr and Grady, 1967; Wakeham et al., 1979; Hites et al., 1980; Louda and Baker, 1984). In contrast, the occurrence of perylene in peats (e.g., Aizenshtat, 1973), soils (e.g., Gocht et al., 2007) and fungi-degraded woods (e.g., Marynowski et al., 2013) supports a terrigenous origin (e.g., Gocht et al., 2007; Itoh and Hanari, 2010; Marynowski et al., 2013).

Perylenequinone pigments are present in many fungi (Weiss et al., 1987; Krohn et al., 1999; Gao et al., 2009) and occasionally in tropical termite nests (Wilcke et al., 2002). These compounds were thought to be a precursor for perylene because of structural similarities (Louda and Baker, 1984). Based on the depth profiles and $\delta^{13}C$ values of PAHs in three Upper Triassic to Middle Jurassic

* Corresponding author at: MOE Key Laboratory for Earth Surface Processes, College of Urban & Environmental Sciences, Peking University, Beijing 100871, China.
E-mail address: yunpingxu@pku.edu.cn (Y. Xu).

sedimentary sequences, Jiang et al. (2000) suggested that fungi were a major contributor for perylene. Itoh et al. (2012) examined the Lake Biwa sediments and catchment soils, and proposed that 4,9-dihydroxyperylene-3,10-quinone (DHPQ) from the soil fungus *Cenococcum geophilum* could be transformed into perylene under natural conditions. However, perylenequinone derivatives have been also found in some marine organisms and thus, an aquatic origin of perylene is also possible (Gao et al., 2009; Kjer et al., 2010).

In this study, we examined the upper 85 m section of the Ocean Drilling Program (ODP) Hole 1202B from the southern Okinawa Trough (OT), which was dated back to the Last Glacial Maximum (LGM). The OT is an ideal venue for studying land–ocean interaction since it receives enormous amounts of continental material from the Yangtze River and other surrounding rivers. In addition, the OT is under a strong influence of the East Asian Monsoon and Kuroshio Current, both playing important roles in hydrological cycle in the densely inhabited East Asia. Our major objectives are to (1) reconstruct variability in the mass accumulation rates of perylene, $C_{37:2}$ alkenone and long chain n-alkanes in the southern OT since the LGM; and (2) identify the source of perylene in the marine environment based on the temporal distribution patterns and stable carbon isotopic compositions of perylene and other biomarkers.

2. Materials and methods

2.1. Samples and age model

The OT is a curved backarc basin located between northwestern Pacific Ocean and southeastern East China Sea (ECS; Fig. 1). It is about 1200 km long and 100–230 km wide with the mean water depth > 1000 m (Salisbury et al., 2002). The OT is subject to the strong influence of the East Asian Monsoon and Kuroshio Current.
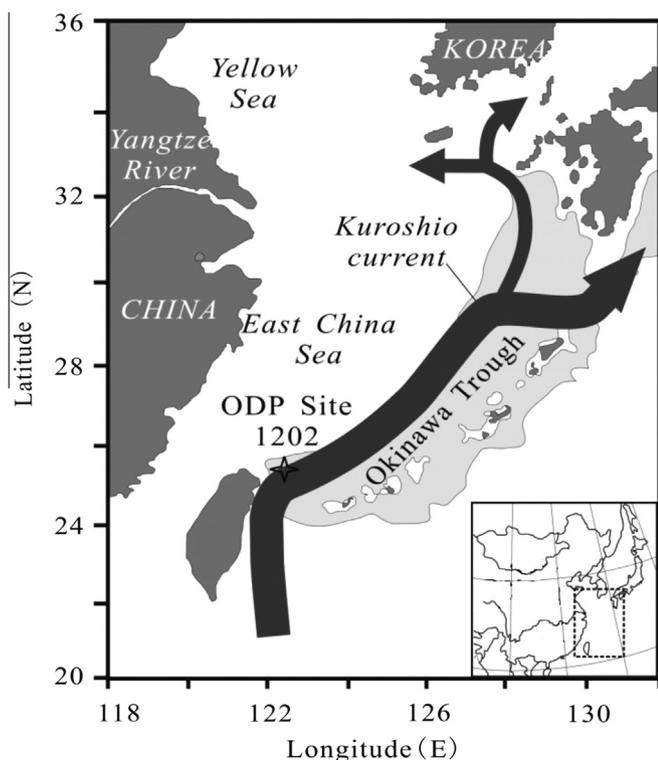

Fig. 1. Location of the ODP Site 1202 in the Okinawa Trough. Black arrows indicate the main axis of Kuroshio Current and its branches.

As the largest warm current in the northwestern Pacific, the Kuroshio Current has a depth up to 1 km and a width of 150–200 km, bringing a large volume of warm and salty water from tropical Pacific to a high latitude ocean (Salisbury et al., 2002).

The ODP Hole 1202B (24°48.24′N, 122°30′E; 1274 m water depth) was drilled during the ODP Leg 195 Expedition in 2001 (Fig. 1). The total length of the core is 140.5 m. In our study, sediments from the top 85 m were investigated. They are exclusively composed of hemipelagic mud without visible silt-sand layer. The clay mineral assemblage mainly consists of illite, chlorite and kaolinite.

The chronology was established on the basis of accelerator mass spectrometry (AMS) ^{14}C dates from Wu et al. (2012) and Wei et al. (2005) (Table 1). The raw ^{14}C dates were converted into calendar years using the CALIB program with a 400 year surface-ocean reservoir correction (Stuiver et al., 1998). The ^{14}C data showed no age reversal and that the upper 85 m of sediment spanned the past ca. 20 kyr. A linear interpolation suggested that the sedimentation rate varied from 2.2 m/kyr in the Holocene to 9.4 m/kyr in the deglaciation (Wei et al., 2005; Wu et al., 2012).

2.2. Lipid analyses

A total of 479 sediment samples were selected for lipid analyses. A detailed method has been described by Sun et al. (2011). Briefly, the sediments were freeze dried and homogenized with a mortar and pestle. About 5 g of sediments were used for lipid extractions. After addition of 3.2 μg squalane as a recovery standard, the sediments were ultrasonically extracted three times, each with 20 ml of dichloromethane:methanol (3:1 v:v) for 15 min. After centrifugation at 3000 rpm for 10 min, the supernatant liquids were concentrated by a rotary evaporator and then completely dried under a mild nitrogen stream. The dried extracts were re-dissolved in 1.0 ml hexane and separated into three fractions using a silica gel column, namely hydrocarbons (5 ml hexane: dichloromethane; 9:1 v:v), ketones (5 ml hexane:dichloromethane; 1:1 v:v) and polar compounds (5 ml dichloromethane: methanol; 1:1 v:v).

Since the coelution of perylene and C_{29} n-alkane exists on the gas chromatograph (GC), a further separation is needed to measure $\delta^{13}C$ of individual compounds. A glass column (30 cm in length, 13 mm i.d.) filled with 12 cm silica gel and 12 cm neutral Al_2O_3 was used. Hydrocarbons were separated into aliphatic hydrocarbons with 45 ml hexane and aromatic hydrocarbons with 50 ml hexane:dichloromethane (1:1 v:v). These two fractions were concentrated prior to instrumental analyses. All solvents used in our study are of the pesticide analysis grade (Dikma Corporation, Beijing, China).

2.3. Gas chromatography-mass spectrometry (GC–MS)

The identification of long chain n-alkanes (C_{25}–C_{33}), aromatic hydrocarbons and long chain alkenones were achieved on an Agilent 7890A–5975C GC–MS system. The ion source was at 250 °C and the ionization energy was 70 eV. A selected ion monitoring (SIM) mode was used with m/z 252 for perylene and m/z 85 for n-alkanes. The separation was carried out on a J&K HP-5MS column (30 m × 0.25 mm i.d., 0.25 μm film thickness). The GC oven temperature was programmed from 60 °C (held 1 min) to 300 °C (held 20 min) at a rate of 6 °C/min. The injection volume was 1 μl in a splitless mode and injection temperature was 300 °C. Helium (> 99.999%) was the carrier gas. Data were acquired and processed with the Chemstation software. The compounds were identified by comparison of mass spectra with authentic standards and the mass library data. The perylene and long chain n-alkanes was quantified on the GC–MS using peak areas based on external

Table 1
AMS ^{14}C dating for planktonic foraminifera in the ODP Hole 1202B.

Depth (mbsf)	^{14}C age (year BP)	Calendar year (BP)	Sedimentation rate (m/kyr)[a]
0.95	580 ± 90	170	5.59
2.90	1150 ± 90	680	3.82
5.15	1880 ± 60	1390	3.17
7.00	2090 ± 120	1630	7.71
9.10	2865 ± 25	2590	2.19
10.88	3153 ± 40	2890	5.93
20.48	5135 ± 45	5490	3.69
31.35	8554 ± 70	8970	3.12
39.35	10,205 ± 55	11,070	3.81
77.35	13340 ± 95	15,110	9.41
83.79	17,110 ± 70	19,750	1.39
88.35	18,480 ± 90	21,330	2.89

[a] Sedimentation rate was calculated according to linear interpolation between two adjacent dating levels.

calibration curves ($R^2 > 0.999$). A mixing standard containing 40–50 ng/μl of three n-alkanes (n-heptadecane n-tricosane, n-hentriacontane), five deuterated PAHs, seventeen PAHs (including perylene) and squalane (Supplementary material) was injected daily to evaluate the reproducibility of the GC–MS.

2.4. GC-FID

Although long chain alkenones were identified by the GC–MS, they were quantified using an Agilent 7890A gas chromatograph coupled to a flame ionization detector (GC–FID) due to the lack of commercial standards. The column was a J&W HP-5 column (30 m × 0.32 mm i.d. × 0.25 μm film thickness). An injection volume was 1 μl. The injection temperature was 300 °C. Helium (purity > 99.999%) was used as carrier gas. The oven was programed from 70 °C (held 1 min) to 250 °C at a rate of 20 °C/min, further increased to 310 °C at a rate of 2 °C/min (held 10 min at 310 °C). The $C_{37:2}$ alkenone was quantified using peak areas by comparison with that of an external standard (perdeuterated n-tetracosane) assuming a relative response factor of 1.

2.5. Compound specific stable carbon detection

Compound specific isotope analyses (CSIA) were carried out on a Finnigan Delta XP isotope ratio mass spectrometry connected to a Finnigan Trace GC. The samples containing n-alkanes and PAHs were injected in a splitless mode (1 μl) at 290 °C. Separation was achieved on a DB–5MS column (60 m × 0.25 mm i.d., film thickness 0.25 μm). The oven temperature program was same as that described for GC–MS (Section 2.3). The samples were run in triplicate. Instrumental performance was verified before and after each sample run using an n-alkane standard mixture with known δ^{13}C values (Chiron, Norway). In this study, we only reported δ^{13}C data with reproducibility better than ± 0.5‰ (standard deviation). The carbon isotope composition was reported in the δ notation (‰) relative to the Vienna Peedee Belemnite (V-PDB) standard.

2.6. Statistical analysis

The analysis of variables in this study was conducted using the program package SPSS 18.0 (Illinois, USA). Kendall's tau correlation coefficient (r) was calculated with a significance level of $p = 0.01$.

3. Result and discussion

3.1. Temporal patterns of perylene since LGM

Perylene, long chain n-alkanes (C_{27}–C_{35}) and $C_{37:2}$ alkenone were detected in most sediments. Since all long chain n-alkanes are derived from leaf waxes of higher plants (Eglinton and Hamilton, 1967), we used C_{31} n-alkane representative of total long chain n-alkanes. Fig. 2 illustrates the five-point running mean of the concentrations and mass accumulation rates (MAR) of perylene, C_{31} n-alkane and $C_{37:2}$ alkenone in the ODP core 1202B. For the past 20 kyr, the perylene accounted for over 90% of total PAHs, consistent with the result for surface sediments in the OT that perylene was the only one predominant PAH detected (Jeng et al., 2003). The concentrations of perylene and C_{31} n-alkane varied from 0.01–1.87 μg/g dws (dry weigh sediment) and 0.10–0.66 μg/g dws, respectively (Fig. 2B and D). The perylene was substantially higher in abundance in the glacial period (∼0.8 μg/g dws from 20–11.5 kyr BP) than in the Holocene (∼0.4 μg/g dws from 11.5 kyr BP to present) (Fig. 2B). A similar temporal pattern was observed for C_{31} n-alkane (Fig. 2D). Unlike perylene and C_{31} n-alkane, $C_{37:2}$ alkenone remained at low concentrations (< 0.6 μg/g dws) during the period of 20–3.0 kyr and reached the maximum (∼1.7 μg/g dws) in late Holocene (Fig. 2F).

Considering large differences in the sedimentation rate among the LGM (ca. 1.4–.9 m/kyr, before 19 kyr BP), the last deglaciation (ca. 9.2 m/kyr from 11 kyr BP to 15 kyr BP) and the Holocene (2.2–7.7 m/kyr from 11 kyr BP to present) (Table 1), we converted the concentration (μg/g dws) into the MAR (μg cm^{-2} yr^{-1}) according to Eq. (1),
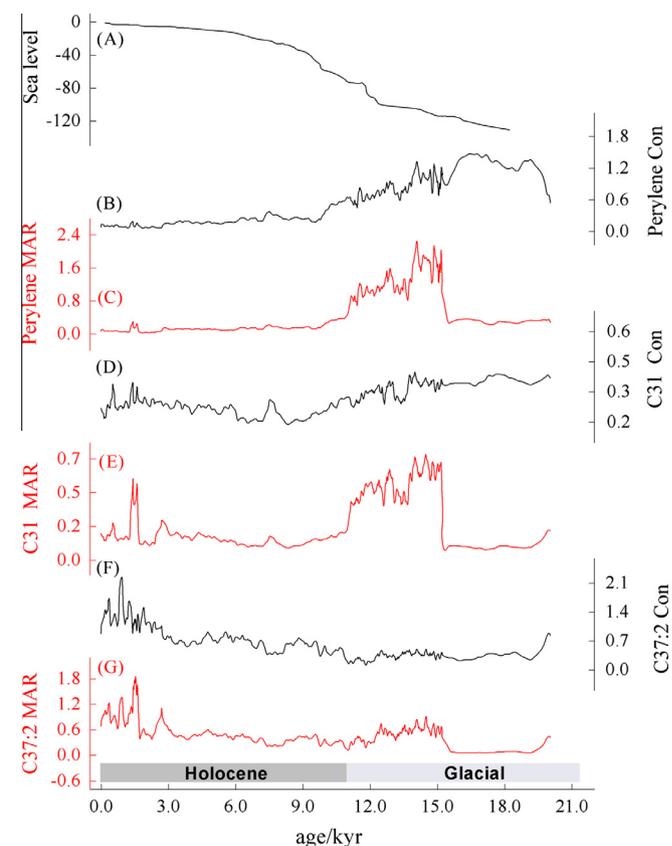
Fig. 2. Variability in concentration (μg/g dws; B, D, F) and mass accumulation rate (MAR; μg cm^{-2} yr^{-1}; C, E, G) of perylene, C_{31} n-alkane and $C_{37:2}$ alkenone in the southern Okinawa Trough over the past 20,000 years, respectively. The data about the global sea level (A) are from Fairbanks (1989).
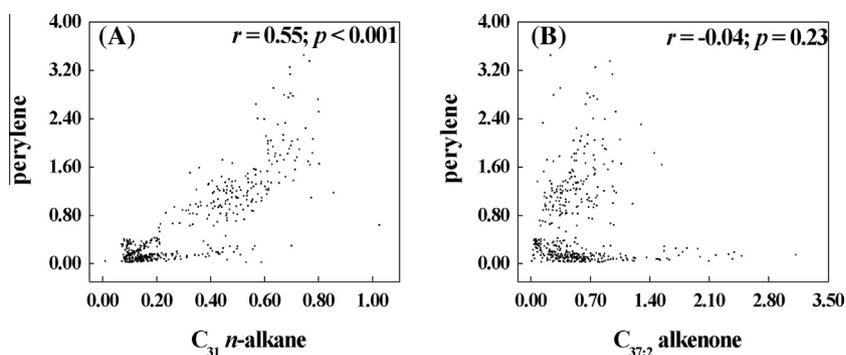
Fig. 3. Kendall correlations of perylene with C_{31} n-alkane (A) and $C_{37:2}$ alkenone (B) in the ODP core 1202B.

$$MAR = \frac{c \times \rho \times \Delta h}{\Delta t} \tag{1}$$

where ρ (g/cm^3) is the density of the raw samples (data from www.iodp.org), Δt (year) is the age difference between two continuous samples (Wei et al., 2005; Wu et al., 2012), Δh (cm) is the depth difference between two continuous samples, and c (μg/g dws) is the concentration of lipid compounds.

The perylene MAR was lower than 0.53 μg cm^{-2} yr^{-1} during the period of 20–15 kyr BP, dramatically increased to 2.0 μg cm^{-2} yr^{-1} and stayed at high levels until ca. 11 kyr BP (Fig. 2C). The perylene MAR rapidly decreased to 0.4 μg cm^{-2} yr^{-1} in early Holocene, and stayed at this low level until present. The MAR of C_{31} n-alkane varied from 0.1–1.0 μg cm^{-2} yr^{-1} (Fig. 2E). A significant correlation between perylene and C_{31} n-alkane ($r = 0.55$; $p < 0.001$; Fig. 3A) suggests that these two compounds share a common origin or their source organisms are controlled by same environmental processes. The MAR of $C_{37:2}$ alkenone remained lower than 0.7 μg cm^{-2} yr^{-1} until 3.0 kyr BP and then increased up to 1.8 μg cm^{-2} yr^{-1} (Fig. 2G). A weak relationship was observed between perylene and $C_{37:2}$ alkenone ($r = -0.04$; $p = 0.23$), reflecting their different sources (Fig. 3B).

3.2. Separation and δ^{13}C measurement of perylene and n-alkanes

Since the Al$_2$O$_3$–SiO$_2$ column was used to purify perylene in hydrocarbon fractions, we evaluated its separation efficiency. The GC–MS chromatograms showed a clear separation of perylene
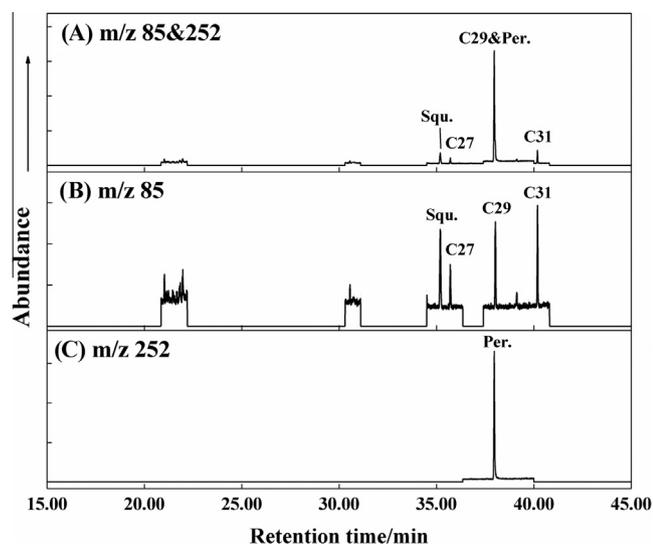

Fig. 4. Representative selected ion monitoring (SIM) chromatograms from (A) Hydrocarbon fraction ($m/z = 85$, 252); (B) Saturate fraction ($m/z = 85$); and (C) Aromatic fraction ($m/z = 252$) for sediments in the ODP core 1202B. Squ.: squalane; C_{27}: n-heptacosane; C_{29}: n-nonacosane; C_{31}: n-hentriacontane; Per.: perylene.

and n-alkanes after passing through the Al$_2$O$_3$–SiO$_2$ column (Fig. 4). The purity of perylene was higher than 95% for all samples except one sediment (1202B-2H-2 85.0–87.0 cm), and the mean recovery of perylene was 71% (39–84%) (Table 2). For long chain n-alkanes, the mean recovery was > 90% and the mean purity was > 90% (Table 2). The CSIA was conducted for 20 sediment samples from the ODP Hole 1202B. The δ^{13}C values of C_{25}–C_{31} n-alkanes were relatively constant throughout the past 20 kyr, falling in a narrow range of −32.7‰ to −28.0‰ (mean of −30.3‰; Table 3). Due to low abundance in the Holocene sediments, the δ^{13}C values of perylene were only reported for those samples from last glacial period (20–11.5 kyr), which varied from −23.6‰ to −22.1‰ with a mean of −22.8‰ (Table 3).

3.3. Source and environmental significance of perylene

In the southern OT, perylene was the dominant PAH throughout the past 20 kyr, suggesting a non-combustion source since the PAHs from oil fuel combustion contain only trace amounts of perylene (Jiang et al., 2000 and references therein). Perylenequinones and their derivatives are components of black pigments in soil or wood-degrading fungi (e.g., Weiss et al., 1987; Wolkenstein et al., 2006; Zhang et al., 2012). In natural environments, especially those

Table 2
Purity and recovery of perylene and long chain n-alkanes after passing through the Al$_2$O$_3$–SiO$_2$ column.

No.	Age (BP)	Perylene		C_{29} n-Alkane		C_{31} n-Alkane	
		A[b]	B[b]	A	B	A	B
1[a]	1400	39.0	97.2	86.3	93.2	82.4	92.9
2	1400	1.2	50.0	108.9	97.5	95.9	98.3
3[a]	3870	50.9	99.7	89.1	64.6	86.6	71.9
4	3920	46.7	99.0	86.6	58.9	97.8	63.1
5[a]	6060	51.9	98.7	99.0	94.6	94.4	97.1
6	6120	56.7	99.6	87.5	98.2	90.3	95.8
7[a]	8790	59.8	99.5	75.8	94.7	94.4	95.7
8	8860	79.9	99.3	94.5	96.3	91.4	94.7
9[a]	10,950	76.3	99.8	80.2	95.2	86.4	72.8
10	11,000	72.5	99.8	88.1	95.6	85.0	94.9
11[a]	11,870	82.2	99.9	86.6	96.4	91.0	97.9
12	11,890	75.9	99.9	96.5	98.9	92.3	98.2
13[a]	12,820	80.5	99.9	88.0	96.1	84.5	94.5
14	12,840	83.3	100.0	100.8	85.3	99.5	86.9
15[a]	13,710	79.9	99.8	91.4	95.7	93.6	97.5
16	13,730	81.8	99.8	88.6	98.8	85.3	99.7
17[a]	14,690	80.4	99.9	88.8	97.4	88.5	99.8
18	14,710	85.2	99.9	89.9	97.5	88.9	99.5
19[a]	17,300	84.8	99.9	91.1	96.5	86.9	99.5
20	17,480	84.4	100.0	84.7	96.8	93.9	99.2
Average		68.8	97.1	90.1	92.4	90.5	92.5

[a] Samples were used for compound specific isotope analysis.
[b] A is recovery (%) while B is purity (%) after passing through the Al$_2$O$_3$–SiO$_2$ column. Recovery (%) was calculated as a mass ratio of analytes after column chromatography over that in initial samples. Purity (%) was defined as the mass ratio of analytes over impurities based on the GC chromatograms.

Table 3
The $\delta^{13}C$ values of long chain n-alkanes and perylene in selected sediments from the ODP core 1202B.

No.	Age (year BP)	$\delta^{13}C$ value of n-alkanes and perylene					
		C_{25}	C_{27}	C_{29}	C_{31}	C_{33}	Per.
1	1400	−29.3 ± 0.2	−30.6 ± 0.3	−30.8 ± 0.1	−31.3 ± 0.2	−32.7 ± 0.4[a]	−[c]
2	3870	−29.0 ± 0.5	−31.0 ± 0.2	−30.1 ± 0.4	−30.0 ± 0.1	−29.4 ± 0.8	−
3	6060	−29.9 ± 1.5[b]	−31.9 ± 0.0	−30.3 ± 0.2	−30.9 ± 0.4	−31.3 ± 0.3[a]	−
4	8790	−29.3 ± 0.1	−30.4 ± 0.2	−30.6 ± 0.2	−30.3 ± 0.1	−31.0 ± 0.1	−
5	10,950	−28.8 ± 0.3[a]	−30.6 ± 1.0[b]	−30.1 ± 0.3	−30.4 ± 0.2	−31.3 ± 0.3[a]	−22.4 ± 0.3
6	11,870	−29.1 ± 0.3	−30.4 ± 0.2	−30.3 ± 0.3	−30.4 ± 0.1	−30.9 ± 0.3	−23.3 ± 0.1
7	12,820	−29.5 ± 0.1	−30.6 ± 0.3	−30.7 ± 0.0	−30.9 ± 0.0	−32.0 ± 0.2	−23.1 ± 0.3
8	13,710	−28.0 ± 0.5	−29.4 ± 0.0	−29.1 ± 0.4	−31.0 ± 0.2	−29.4 ± 1.0[b]	−22.2 ± 0.2
9	14,690	−29.6 ± 0.4	−30.6 ± 0.4	−30.6 ± 0.1	−30.8 ± 0.1	−31.1 ± 0.1	−23.6 ± 0.0[a]
10	17,300	−28.8 ± 0.3	−29.5 ± 0.3	−30.2 ± 0.0	−30.6 ± 0.1	−30.7 ± 0.6[b]	−22.1 ± 0.3

[a] Peak intensity was lower than 500 mV.
[b] Standard error was > 0.5.
[c] Compounds were too low abundant to be measured accurately for $\delta^{13}C$.

with rapid deposition, anoxic conditions, perylenequinones can be transformed into perylene (Itoh et al., 2012; Marynowski et al., 2013). Consequently, fungi have been thought to be a major biological source for perylene in continental environments (Wilcke et al., 2002; Bechtel et al., 2007; Gocht et al., 2007). However, the source of perylene in aquatic environments remains elusive, assigned as either an allochthonous organic matter from terrigenous organisms (Itoh et al., 2012; Bertrand et al., 2013), an autochthonous contributor from algae (Wakeham et al., 1979; Venkatesan, 1988), or an in situ diagenetic product from non-specific precursor (Silliman et al., 1998; Fan et al., 2011). Such complexity is particularly true for river influenced, marginal seas where significant amounts of terrigenous and marine organic matter mix.

As a regional depocenter, the southern OT receives large amounts of terrigenous materials from surrounding areas (Salisbury et al., 2002; Diekmann et al., 2008). The Yangtze River delivers a total of 240–680 Mt of sediments per year to the East China Sea, small portions of which can reach the southern OT (Liu et al., 2007). In addition, the Lanyang-Hsi, a mountainous river in the northeastern Taiwan Island with the mouth directly situated adjacent to the southern OT, transports 6–9 Mt sediments per year into the OT (Kao et al., 2003; Diekmann et al., 2008). Zhang et al. (2012) detected perylenequinones in a fungus species, *Alternaria sp. M6*, collected from coastal soils in the eastern China. Given these facts, perylene and derivatives from soil fungi may be transported into rivers and then flow into the southern OT. Such hypothesis is corroborated by a strong correlation of perylene with C_{31} n-alkane, a biomarker for terrigenous plants (Eglinton and Hamilton, 1967) and a weak correlation of perylene with $C_{37:2}$ alkenone, a biomarker for marine planktonic algae from the Class Prymnesiophyceae (Volkman et al., 1980).

Additional evidence to support the terrigenous origin for perylene is from carbon stable isotope compositions (Hayes et al., 1990; Collister et al., 1994). For the past 20 kyr, the mean $\delta^{13}C$ value of C_{31} n-alkane was −30.2‰, presenting a typical value for C3 plants (Collister et al., 1994). Such assignment agrees well with C3 plants dominating the distribution in the Yangtze River basin and the Lanyang-Hsi watershed, two major corridors for transporting terrigenous materials into the southern OT (Diekmann et al., 2008). Compared to C_{31} n-alkane, perylene was apparently enriched in ^{13}C (−23.6‰ to −22.1‰ for $\delta^{13}C$), reflecting different precursors between these two compounds. It has been reported that soil organic matter rather than plant detritus is the majority composition of terrigenous organic matter in the Yangtze River (Yang et al., 2008). Tan et al. (1991) reported that the $\delta^{13}C_{org}$ values of particulate organic matter were −24‰ to −26‰ in the Yangtze River estuary. Particulate organic matter in the Lanyang-Hsi watersheds had

a mean $\delta^{13}C_{org}$ value of −25.5‰ ± 0.3‰, similar to that in other major rivers in Taiwan (Kao et al., 2003). The relatively heavier $\delta^{13}C_{org}$ of fluvial organic matter compared to C3 terrigenous plants (−27‰) can be attributed to a decomposition effect which causes a positive $\delta^{13}C$ shift by 2–3‰ from fresh vegetation to deeper soil organic matter (Wang et al., 2008). Furthermore, saprotrophic fungi have been observed to be enriched in ^{13}C by ∼2‰ relative to their carbon sources probably due to specific carbon fractionation during lignin or cellulose degradation (Zeller et al., 2007). Taking these factors together, we can explain why perylene from soil fungi has a more positive $\delta^{13}C$ value by 4–5‰ than bulk organic matter in C3 plants.

For the past 20 kyr, the maximum perylene MAR occurred in the deglaciation from ∼15–11 kyr BP (Fig. 2C), coeval with rapid global sea level rise (Fig. 2A) (Fairbanks, 1989; Bard et al., 1990). This deglaciation period is characterized by the highest sedimentation rate in the southern OT (9.4 m/kyr; Table 1). From the LGM (ca. 20–18 kyr BP) to the deglaciation (ca. 18–11.5 kyr BP), climate became more humid, increasing fluvial runoffs of the Yangtze River and other small rivers. Meanwhile, the sea level rise submerged the East China Sea shelf and caused strong sediment reworking. As a result, more terrigenous materials (including soil organic matter and perylene) were transported from the China mainland and the East China Sea shelf into the southern OT, resulting in higher perylene abundance in marine sediments.

4. Conclusion

We have reconstructed high resolution records of perylene, C_{31} n-alkane and long chain alkenones in the southern OT for the last 20,000 years. The concentrations of perylene, C_{31} n-alkane and $C_{37:2}$ alkenone ranged from 0.01–1.87 µg/g dws, 0.10–0.66 µg/g dws and 0.0–3.97 µg/g dws, respectively. The mass accumulation rate of perylene was substantially higher in the deglaciation than the Holocene and LGM, synchronous with the rapid global sea level rise. Perylene presents a strong correlation with C_{31} n-alkane ($r = 0.55$, $p < 0.001$) and a weak correlation with long chain alkenones ($r = -0.04$, $p = 0.23$). The mean $\delta^{13}C$ value of perylene (-22.8‰ ± 0.6‰) was remarkably higher than that of long chain n-alkanes (−30.7‰ ± 0.4‰), but was close to that of particulate organic matter in adjacent rivers such as the Yangtze River and mountainous rivers (−24‰ to −25‰). Based on these findings, we attributed perylene in the OT to a terrigenous origin likely from soil fungi. A close relationship of perylene with the terrigenous biomarker and the sedimentation rate supports perylene as a potential tracer for terrigenous organic carbon in marine

environments. Future study will be for perylene in terrigenous/aquatic and oxic/anoxic environments in order to better understand the transformation mechanism from the biological precursors to perylene.

Acknowledgments

Appendix A. Supplementary material

Supplementary data associated with this article can be found, in the online version, at http://dx.doi.org/10.1016/j.orggeochem.2014.09.008.

Associate Editor—**Ian Bull**

References

Aizenshtat, Z., 1973. Perylene and its geochemical significance. Geochimica et Cosmochimica Acta 37, 559–567.

Bard, E., Hamelin, B., Fairbanks, R.G., 1990. U–Th ages obtained by mass spectrometry in corals from Barbados: sea level during the past 130,000 years. Nature 346, 456–458.

Baumard, P., Budzinski, H., Michon, Q., Garrigues, P., Burgeot, T., Bellocq, J., 1998. Origin and bioavailability of PAHs in the Mediterranean Sea from mussel and sediment records. Estuarine, Coastal and Shelf Science 47, 77–90.

Bechtel, A., Widera, M., Sachsenhofer, R.F., Gratzer, R., Luecke, A., Woszczyk, M., 2007. Biomarker and stable carbon isotope systematics of fossil wood from the second Lusatian lignite seam of the Lubstow deposit (Poland). Organic Geochemistry 38, 1850–1864.

Bertrand, O., Montargès-Pelletier, E., Mansuy-Huault, L., Losson, B., Faure, P., Michels, R., Pernot, A., Arnaud, F., 2013. A possible terrigenous origin for perylene based on a sedimentary record of a pond (Lorraine, France). Organic Geochemistry 58, 69–77.

Collister, J.W., Rieley, G., Stern, B., Eglinton, G., Fry, B., 1994. Compound-specific δ¹³C analyses of leaf lipids from plants with differing carbon dioxide metabolisms. Organic Geochemistry 21, 619–627.

Diekmann, B., Hofmann, J., Henrich, R.I., Futterer, D.K., Rohl, U., Wei, K.Y., 2008. Detrital sediment supply in the southern Okinawa Trough and its relation to sea-level and Kuroshio dynamics during the late Quaternary. Marine Geology 255, 83–95.

Eglinton, G., Hamilton, R.J., 1967. Leaf epicuticular waxes. Science 156, 1322–1335.

Fairbanks, R.G., 1989. A 17,000-year glacio-eustatic sea level record: Influence of glacial melting rates on the Younger Dryas event and deep-ocean circulation. Nature 342, 637–642.

Fan, C.-W., Shiue, J., Wu, C.-Y., Wu, C.-Y., 2011. Perylene dominance in sediments from a subtropical high mountain lake. Organic Geochemistry 42, 116–119.

Gao, S.S., Li, X.M., Wang, B.G., 2009. Perylene derivatives produced by Alternaria alternata, an endophytic fungus isolated from Laurencia species. Natural Product Communications 4, 1477–1480.

Gocht, T., Barth, J.A.C., Epp, M., Jochmann, M., Blessing, M., Schmidt, T.C., Grathwohl, P., 2007. Indications for pedogenic formation of perylene in a terrestrial soil profile: depth distribution and first results from stable carbon isotope ratios. Applied Geochemistry 22, 2652–2663.

Grice, K., Lu, H., Atahan, P., Asif, M., Hallmann, C., Greenwood, P., Maslen, E., Tulipani, S., Williford, K., Dodson, J., 2009. New insights into the origin of perylene in geological samples. Geochimica et Cosmochimica Acta 73, 6531–6543.

Gschwend, P.M., Hites, R.A., 1981. Fluxes of polycyclic aromatic-hydrocarbons to marine and lacustrine sediments in the northeastern United States. Geochimica et Cosmochimica Acta 45, 2359–2367.

Gschwend, P.M., Chen, P.H., Hites, R.A., 1983. On the formation of perylene in recent sediments – kinetic-models. Geochimica et Cosmochimica Acta 47, 2115–2119.

Hayes, J.M., Freeman, K.H., Popp, B.N., Hoham, C.H., 1990. Compound-specific isotopic analyses: a novel tool for reconstruction of ancient biogeochemical processes. Organic Geochemistry 16, 1115–1128.

Hites, R.A., Laflamme, R.E., Windsor Jr., J.G., Farrington, J.W., Deuser, W.G., 1980. Polycyclic aromatic hydrocarbons in an anoxic sediment core from the Pettaquamscutt River (Rhode Island, USA). Geochimica et Cosmochimica Acta 44, 873–878.

Ishiwatari, R., Ogura, K., Horie, S., 1980. Organic geochemistry of a lacustrine sediment (Lake Haruna, Japan). Chemical Geology 29, 261–280.

Itoh, N., Hanari, N., 2010. Possible precursor of perylene in sediments of Lake Biwa elucidated by stable carbon isotope composition. Geochemical Journal 44, 161–166.

Itoh, N., Sakagami, N., Torimura, M., Watanabe, M., 2012. Perylene in Lake Biwa sediments originating from *Cenococcum geophilum* in its catchment area. Geochimica et Cosmochimica Acta 95, 241–251.

Jeng, W.-L., Lin, S., Kao, S.-J., 2003. Distribution of terrigenous lipids in marine sediments off northeastern Taiwan. Deep Sea Research Part II: Topical Studies in Oceanography 50, 1179–1201.

Jiang, C., Alexander, R., Kagi, R.I., Murray, A.P., 2000. Origin of perylene in ancient sediments and its geological significance. Organic Geochemistry 31, 1545–1559.

Kao, S., Lin, F., Liu, K., 2003. Organic carbon and nitrogen contents and their isotopic compositions in surficial sediments from the East China Sea shelf and the southern Okinawa Trough. Deep Sea Research Part II: Topical Studies in Oceanography 50, 1203–1217.

Kjer, J., Debbab, A., Aly, A.H., Proksch, P., 2010. Methods for isolation of marine-derived endophytic fungi and their bioactive secondary products. Nature Protocols 5, 479–490.

Krohn, K., John, M., Aust, H.-J., Draeger, S., Schulz, B., 1999. Biologically active metabolites from fungi 131 Stemphytriol, a new perylene derivative from *Monodictys fluctuata*. Natural Product Letters 14, 31–34.

Laflamme, R.E., Hites, R.A., 1978. Global distribution of polycyclic aromatic-hydrocarbons in recent sediments. Geochimica et Cosmochimica Acta 42, 289–303.

Liu, J., Xu, K., Li, A.e.a., Milliman, J., Velozzi, D., Xiao, S., Yang, Z., 2007. Flux and fate of Yangtze River sediment delivered to the East China Sea. Geomorphology 85, 208–224.

Louda, J.W., Baker, E.W., 1984. Perylene occurrence, alkylation and possible sources in deep-ocean sediments. Geochimica et Cosmochimica Acta 48, 1043–1058.

Marynowski, L., Smolarek, J., Bechtel, A., Philippe, M., Kurkiewicz, S., Simoneit, B.R.T., 2013. Perylene as an indicator of conifer fossil wood degradation by wood-degrading fungi. Organic Geochemistry 59, 143–151.

Orr, W.L., Grady, J.R., 1967. Perylene in basin sediments off southern California. Geochimica et Cosmochimica Acta 31, 1201–1209.

Salisbury, M.H., Shinohara, M., Richter, C., 2002. Proc. ODP, Init. Repts., 195: College Station, TX (Ocean Drilling Program). http://dx.doi.org/10.2973/odp.proc.ir.195.2002.

Silliman, J.E., Meyers, P.A., Eadie, B.J., 1998. Perylene: an indicator of alteration processes or precursor materials? Organic Geochemistry 29, 1737–1744.

Silliman, J., Meyers, P., Ostrom, P., Ostrom, N., Eadie, B., 2000. Insights into the origin of perylene from isotopic analyses of sediments from Saanich Inlet, British Columbia. Organic Geochemistry 31, 1133–1142.

Silliman, J.E., Meyers, P.A., Eadie, B.J., Val Klump, J., 2001. A hypothesis for the origin of perylene based on its low abundance in sediments of Green Bay, Wisconsin. Chemical Geology 177, 309–322.

Soclo, H., Garrigues, P., Ewald, M., 2000. Origin of polycyclic aromatic hydrocarbons (PAHs) in coastal marine sediments: case studies in Cotonou (Benin) and Aquitaine (France) areas. Marine Pollution Bulletin 40, 387–396.

Stuiver, M., Reimer, P.J., Bard, E., Beck, J.W., Burr, G.S., Hughen, K.A., Kromer, B., McCormac, G., Van der Plicht, J., Spurk, M., 1998. INTCAL98 radiocarbon age calibration, 24,000–0 cal BP. Radiocarbon 40, 1041–1083.

Sun, D., Tan, W., Pei, Y., Zhou, L., Wang, H., Yang, H., Xu, Y., 2011. Late Quaternary environmental change of Yellow River Basin: an organic geochemical record in Bohai Sea (North China). Organic Geochemistry 42, 575–585.

Tan, F.C., Cai, D.L., Edmond, J.M., 1991. Carbon isotope geochemistry of the Changjiang estuary. Estuarine, Coastal and Shelf Science 32, 395–403.

Venkatesan, M., 1988. Occurrence and possible sources of perylene in marine sediments – a review. Marine Chemistry 25, 1–27.

Volkman, J.K., Eglinton, G., Corner, E.D.S., Forsberg, T.E.V., 1980. Long-chain alkenes and alkenones in the marine coccolithophorid Emiliania huxleyi. Phytochemistry 19, 2619–2622.

Wakeham, S.G., Schaffner, C., Giger, W., Boon, J.J., De Leeuw, J., 1979. Perylene in sediments from the Namibian Shelf. Geochimica et Cosmochimica Acta 43, 1141–1144.

Wakeham, S.G., Schaffner, C., Giger, W., 1980. Polycyclic aromatic-hydrocarbons in recent lake-sediments 2. Compounds derived from biogenic precursors during early diagenesis. Geochimica et Cosmochimica Acta 44, 415–429.

Wang, G., Feng, X., Han, J., Zhou, L., Tan, W., Su, F., 2008. Paleovegetation reconstruction using δ¹³C of soil organic matter. Biogeosciences 5, 1325–1337.

Wei, K.Y., Mii, H.S., Murray, C.-Y., 2005. Age model and oxygen isotope stratigraphy of site ODP1202 in the southern Okinawa Trough, northwestern pacific. Terrestrial Atmospheric and Oceanic Sciences 16, 1–17.

Weiss, U., Merlini, L., Nasini, G., 1987. Naturally occurring perylenequinones. Fortschritte der Chemie organischer Naturstoffe/Progress in the Chemistry of Organic Natural Products. Springer, pp. 1–71.

Wilcke, W., Krauss, M., Amelung, W., 2002. Carbon isotope signature of polycyclic aromatic hydrocarbons (PAHs): evidence for different sources in tropical and temperate environments? Environmental Science & Technology 36, 3530–3535.

Wilcke, W., Amelung, W., Krauss, M., Martius, C., Bandeira, A., Garcia, M., 2003. Polycyclic aromatic hydrocarbon (PAH) patterns in climatically different ecological zones of Brazil. Organic Geochemistry 34, 1405–1417.

Wolkenstein, K., Gross, J.H., Falk, H., Schöler, H.F., 2006. Preservation of hypericin and related polycyclic quinone pigments in fossil crinoids. Proceedings of the Royal Society B: Biological Sciences 273, 451–456.

Wu, W.C., Tan, W.B., Zhou, L.P., Yang, H., Xu, Y.P., 2012. Sea surface temperature variability in southern Okinawa Trough during last 2700 years. Geophysical Research Letters 39, L14705. http://dx.doi.org/10.1029/2012gl052749.

Yang, L., Wu, Y., Zhang, J., Yu, H., Zhang, G., Zhu, Z., 2008. Distribution of lignin and sources of organic matter in surface sediments from the adjacent area of the Changjiang Estuary in China. Acta Oceanologica Sinica 30, 35–42.

Zeller, B., Brechet, C., Maurice, J.-P., Tacon, F., 2007. ^{13}C and ^{15}N isotopic fractionation in trees, soils and fungi in a natural forest stand and a Norway spruce plantation. Annals of Forest Science 64, 419–429.

Zhang, S.-Y., Li, Z.-L., Bai, J., Wang, Y., Zhang, L.-M., Wu, X., Hua, H.-M., 2012. A new perylenequinone from a halotolerant fungus, *Alternaria* sp. M6. Chinese Journal of Natural Medicines 10, 68–71.